

# Ultra-Efficient Interleaved Vertical-Junction Microdisk Modulator with Integrated Heater

Asher Novick<sup>1,\*,\dagger</sup>, Songli Wang<sup>1</sup>, Anthony Rizzo<sup>2</sup>, Vignesh Gopal<sup>1</sup>,  
and Keren Bergman<sup>1</sup>

<sup>1</sup>Department of Electrical Engineering, Columbia University, New York, NY, 10027, USA

<sup>2</sup>Air Force Research Laboratory Information Directorate, Rome, NY, 13441, USA

<sup>\dagger</sup>Now at Xscape Photonics

\*asher.novick@columbia.edu

**Abstract:** We demonstrate a vertical-junction microdisk modulator with interleaved RF contacts and doped-silicon heater. We measure a resonance ER=36.5 dB, FSR=27.15 nm, and open eye diagrams at 32 Gb/s NRZ with 800 mV peak-to-peak driving signal. © 2024 The Author(s)

## 1. Introduction & Background

Integrated resonant modulators are an attractive alternative to more traditional Mach-Zehnder Interferometer (MZI) based modulators, as the resonator field enhancement allows for a more compact footprint, compatibility with cutting-edge complementary metal-oxide-semiconductor (CMOS) node driving voltages, and substantially lower energy consumption [1]. This is particularly true in the case of dense wavelength division multiplexing (DWDM) systems, where the resonant modulator's inherent wavelength selectivity enables several modulators to be coupled to a single bus waveguide carrying multiple wavelengths, reducing the need for separate wavelength multiplexing and de-multiplexing link components, as shown in Fig. 1a [2]. Each resonator in this cascaded array can then independently modulate its corresponding wavelength, with negligible cross-talk between spectral channels. Multiple styles of resonant modulators have emerged, but vertical-junction (VJ) microdisk modulators are the most promising that are compatible with standard CMOS foundry fabrication processes. In contrast to a lateral- or interleaved-junction microring modulator, VJ microdisk modulators overlap a highly confined and high internal quality factor (Q) whispering gallery mode with a vertically oriented PN diode. This combination offers unparalleled modulation efficiency, due to the increased resonator free spectral range (FSR) and depletion response (measured in GHz/V) [1, 2].

Here, we propose and demonstrate a VJ microdisk modulator with co-radial interleaved RF contacts which incorporates an efficient interior doped silicon heater. The proposed modulator is fabricated on 300 mm wafer in a commercial foundry and only requires four doping implants to form the contact regions (P++ and N++) and VJ (P and N) diode. The resonator shows a deep resonance extinction ratio (ER) of 36.5 dB, wide FSR of 27.15 nm, and high thermal tuning efficiency of  $\approx 0.3$  nm/mW. To demonstrate the device's modulation bandwidth and efficiency, an open eye diagram with optical modulation amplitude (OMA)  $\approx 200$   $\mu$ W at 32 Gb/s non-return to zero (NRZ) with 800 mV peak-to-peak driving signal is measured. The demonstrated device metrics satisfy the stringent performance requirements of future high bandwidth, low energy DWDM silicon photonic links.

## 2. Interleaved RF Contact Design

The microdisk whispering gallery mode necessitates that all electrical contacts be placed within the external radius of modulator, as there must be a clean full etch at this boundary to ensure radiative bend loss does not degrade the resonator Q, especially for large FSR designs permitting high channel count DWDM [2, 3]. Foundry design rules regarding minimum spacing between metal layers forces the series resistance component of the microdisk modulator RC bandwidth to become increasingly constrained as the radius decreases [4, 5]. These limitations are exacerbated with the inclusion of an integrated heater, which requires room for an additional two electrical contacts within an already limited area. The largest FSR disk and ring modulators proposed often forgo an integrated heater, making them impractical for actual integration within DWDM links where fine tuning of the resonance location during operation is necessary [1, 5].

Figure 1b illustrates our proposed VJ microdisk modulator interleaved contact scheme relative to the left-right contact scheme often shown in literature [5]. Larger  $N$ , where  $N$  is the number of parallel RF contacts, results in the RC modulation bandwidth and modulation efficiency of a VJ microdisk modulator to be increased, analogous to how interleaved lateral junction ring modulators contacts are arranged [6]. Figure 1c illustrates a simplified small

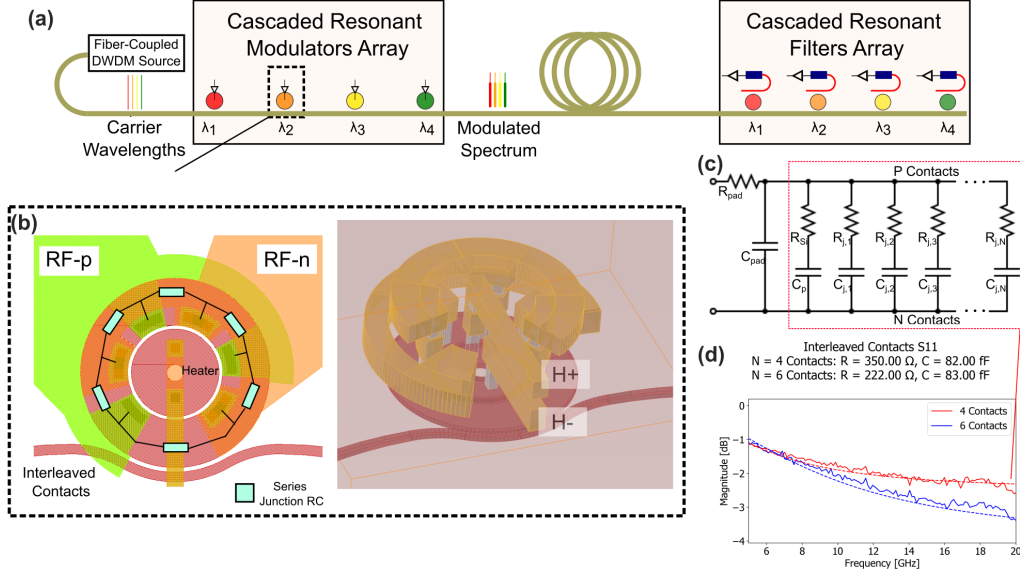


Fig. 1. (a) Schematic of exemplary 4 wavelength resonator driven DWDM interconnect. (b) Top and perspective view illustrations of the proposed interleaved contact scheme ( $N = 6$ ). (c) Simplified small signal model for the modulator with  $N$  interleaved contacts, with  $R_{\text{pad}}$  being the series resistance of the pads,  $C_{\text{pad}}$  being the capacitance of the pads, and the parallelized junction series impedance represented by  $R_j$  and  $C_j$ . (d) The measured S11 frequency response after de-embedding the pads and connected metal traces, showing reduction in back reflection due to greater impedance matching with greater number of parallel interleaved contacts.

signal model from pads to device for an  $N$  parallel interleaved contact scheme microdisk modulator. Figure 1d plots the measured S11 frequency response and model fit for a fabricated  $N = 4$  and  $N = 6$  interleaved contact scheme after de-embedding the probe pads and metal traces to the modulator. With more parallel contacts for the same disk radius, the VJ series resistance reduces as expected, suggesting higher modulation bandwidth and reduced electrical back reflections.

### 3. Optical Characterization and Modulation

Figure 2a shows an annotated micrograph of the proposed microdisk modulator design, fabricated on a photonic integrated circuit (PIC) through the AIM SUNY foundry. Figure 2b plots the spectral transmission showing  $\text{ER} = 36.5$  dB,  $Q \approx 6,000$ , and  $\text{FSR} = 27.15$  nm, with higher order modes suppressed across the full C-band. The DC depletion response was also measured as 7.3 GHz/V, in-line with typical VJ modulators [1, 2]. Figure 2c shows the thermal tuning efficiency to be 0.3 nm/mW.

Figure 2d shows the schematic for the characterization and modulation experimental setup. Modulation was driven by an Anritsu MP1900A Pulse Pattern Generator (PPG) with a NRZ pseudo-random bit sequence  $2^{15} - 1$  bits long (PRBS15) and peak-to-peak voltage of 800 mV. A HyperLabs HL9447 Bias Tee connected the PPG to the modulators RF input and a DC reverse bias of -1.2 V is applied to the modulator by a DC power supply. A Keysight 81606A tunable laser source (TLS) sends light at 1556.44 nm into the integrated modulator via a single mode fiber (SMF) coupled grating coupler, after passing through a polarization controller (PC) for optimizing insertion loss (IL) through the PIC. The modulated carrier wavelength is coupled back into SMF and amplified through an erbium doped fiber amplifier (EDFA) before being measured by a Keysight N1092C sampling oscilloscope, with a Thorlabs EVOA1550A variable optical attenuator (VOA) placed before the optical input. The oscilloscope receives a clock trigger directly from the PPG and is set to pattern lock on the 32 Gb/s NRZ PRBS15 pattern. Figure 2e shows a completely open eye diagram captured by the oscilloscope with  $\text{OMA} \approx 200 \mu\text{W}$ , indicating the device's high modulation bandwidth and efficiency.

### 4. Conclusion

In this work, we have demonstrated an ultra-efficient high speed microdisk modulator with a deep ER and wide FSR, fully compatible with commercial foundry processes and only requiring four distinct doping implants. Despite the wide FSR, the design includes room for an integrated doped silicon heater, allowing for efficient fine tun-

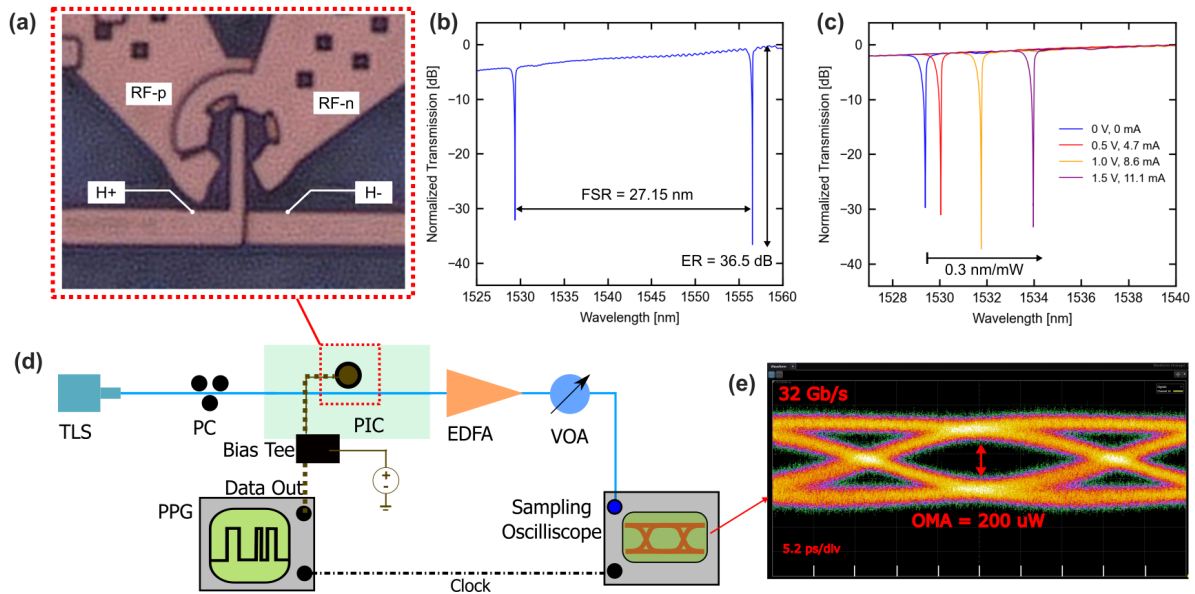


Fig. 2. (a) Micrograph of the fabricated interleaved contact microdisk modulator. (b) Spectral transmission showing  $ER = 36.5$  dB,  $Q \approx 6,000$ , and  $FSR = 27.15$  nm, with higher order modes suppressed across the full C-band. (c) Thermal tuning efficiency measurement, showing  $\lambda = 0.3$  nm/mW. (d) Schematic of modulation experiment. (e) Open eye diagram at 32 Gb/s with PRBS15, driving voltage of 800 mV peak-to-peak, and  $OMA \approx 200$   $\mu$ W.

ing of resonance location during operation. Furthermore, this design is fully compatible with prior demonstrated wafer-scale undercut techniques in the same foundry process, which have been shown to increase comparable resonator thermal tuning efficiency by greater than  $3 \times$  [7]. The underlying design can be scaled to further reduced radii while maintaining the same number of parallel contacts, with  $FSR > 30$  nm possible without any change in foundry design rules. The proposed and demonstrated disk modulator design offers a viable path forward towards realizing ultra-efficient integrated DWDM interconnects, with unprecedented bandwidth density and fabricated at commercial scale [2].

## References

1. E. Timurdogan *et al.*, "An ultralow power athermal silicon modulator," *Nat. communications* **5**, 1–11 (2014).
2. A. Rizzo *et al.*, "Massively scalable kerr comb-driven silicon photonic link," *Nat. Photonics* **17**, 781–790 (2023).
3. N. Eid *et al.*, "Wide fsr silicon-on-insulator microring resonator with bent couplers," in *2015 IEEE 12th International Conference on Group IV Photonics (GFP)*, (2015), pp. 96–97.
4. M. M. Tarar *et al.*, "Design and implementation of an electrical interface for ring modulators using cpws," in *GeMiC 2014; German Microwave Conference*, (2014), pp. 1–4.
5. A. Biberman *et al.*, "Adiabatic microring modulators," *Opt. Express* **20**, 29223–29236 (2012).
6. L. Alloatti, D. Cheian, and R. J. Ram, "High-speed modulator with interleaved junctions in zero-change cmos photonics," *Appl. Phys. Lett.* **108** (2016).
7. A. Rizzo *et al.*, "Ultra-efficient foundry-fabricated resonant modulators with thermal undercut," in *CLEO 2023*, (Optical Publishing Group, 2023), p. SF2K.6.

**Acknowledgements:** This work was supported in part by the U.S. Advanced Research Projects Agency–Energy under ENLITENED Grant DE-AR000843, and in part by the U.S. Defense Advanced Research Projects Agency under Photonics in the Package for Extreme Scalability (PIPES) Grant HR00111920014.